

General Disclaimer

One or more of the Following Statements may affect this Document

- This document has been reproduced from the best copy furnished by the organizational source. It is being released in the interest of making available as much information as possible.
- This document may contain data, which exceeds the sheet parameters. It was furnished in this condition by the organizational source and is the best copy available.
- This document may contain tone-on-tone or color graphs, charts and/or pictures, which have been reproduced in black and white.
- This document is paginated as submitted by the original source.
- Portions of this document are not fully legible due to the historical nature of some of the material. However, it is the best reproduction available from the original submission.

**NASA TECHNICAL
MEMORANDUM**

NASA TM-78858

(NASA-TM-78858) PULSE IGNITION
CHARACTERIZATION OF MERCURY ION THRUSTER
HOLLOW CATHODE USING AN IMPROVED PULSE
IGNITOR (NASA) 20 p HC A02/MF A01 CSCL 21C

N78-21203

Unclas
12410

G3/20

NASA TM-78858

**PULSE IGNITION CHARACTERIZATION OF MERCURY ION THRUSTER
HOLLOW CATHODE USING AN IMPROVED PULSE IGNITOR**

by E. G. Wintucky and R. P. Gruber
Lewis Research Center
Cleveland, Ohio 44135

TECHNICAL PAPER to be presented at the
Thirteenth International Electric Propulsion Conference
cosponsored by the American Institute of Aeronautics and Astronautics
and the Deutsche Gesellschaft fur Luft-und Raumfahrt
San Diego, California, April 25-27, 1978



PULSE IGNITION CHARACTERIZATION OF MERCURY ION THRUSTER

HOLLOW CATHODE USING AN IMPROVED PULSE IGNITOR

by E. G. Wintucky and R. P. Gruber

National Aeronautics and Space Administration
Lewis Research Center
Cleveland, Ohio 44135

SUMMARY

An investigation of the high voltage pulse ignition characteristics of the 8-cm mercury ion thruster neutralizer cathode identified a low rate of voltage rise and long pulse duration as desirable factors for reliable cathode starting. Cathode starting breakdown voltages were measured over a range of mercury flow rates and tip heater powers for pulses with five different rates of voltage rise. Breakdown voltage requirements for the fastest rising pulse (2.5 to 3.0 kV/ μ sec) were substantially higher (2 kV or more) than for the slowest rising pulse (0.3 to 0.5 kV/ μ sec) for the same starting conditions. This paper also describes an improved, low impedance pulse ignitor circuit which reduces power losses and eliminates problems with control and packaging associated with earlier designs.

INTRODUCTION

The 8-cm mercury ion thruster (refs. 1 and 2) has been developed for a variety of auxiliary propulsion functions. One requirement is to perform 2500 or more on-off duty cycles over a mission lifetime. Rapid and reliable restart capability is a crucial requirement for applications of this thruster.

The hollow cathodes in the cathode-isolator-vaporizer (CIV) and neutralizer-isolator-vaporizer (NIV) assemblies play major roles in ion thruster start-up and operation. High voltage pulse ignition is now well established as a useful method for hollow cathode starting (refs. 3 to 5) and is the approach taken in the 8-cm ion thruster subsystem planned for flight test (ref. 6). To assure reliable cathode starting and to define acceptable regions of operation and power processor requirements, it is important to identify those parameters which control start-up.

The high voltage pulse ignition characteristics of two 8-cm ion thruster neutralizer cathodes were investigated using pulses with five different rates of voltage rise. Breakdown voltages were measured over a range of Hg flow rates and cathode tip heater powers. The focus of this investigation was on predischARGE ignition characteristics. Experi-

ence has shown that breakdown almost invariably results in a sustainable discharge. This paper presents the results of the high voltage pulse ignition tests and identifies desirable factors for reliable cathode start-up.

Also described in the paper is a low impedance pulse ignitor circuit which was used in the determination of pulse ignition characteristics. The low impedance pulse ignitor reduced power losses and eliminated problems with control and packaging associated with earlier designs. The low impedance was made possible by a substantial reduction in pulse duration. The improved pulser concept has been incorporated in the present 8-cm Engineering Model Thruster (EMT) system (ref. 7). The pulse characteristics found desirable for reliable cathode starting do not necessarily correspond to a minimum weight circuit design. Trade offs with transformer size and weight and circuit complexity are discussed in the paper.

APPARATUS

High Voltage Pulse Ignitor

The low impedance pulse ignitor operates similarly to those used previously for hollow cathode starting (refs. 3 to 5). An energy storage capacitor is discharged across the primary of a step-up transformer. The positive high voltage output is delivered to the keeper electrode together with approximately 50 V dc from the keeper supply to provide discharge maintenance.

Two high voltage pulse circuit configurations used in the past are shown in figure 1. Both configurations require blocking diodes in series with the output of the keeper supply. In figure 1(b) the diode provides a path around the secondary winding for the discharge maintenance current. A number of disadvantages result from this arrangement. One of the most serious disadvantages is the continuous diode power loss during cathode operation. For the neutralizer cathode alone, the diode power loss amounts to 3 W or more. For typical applications of the 8-cm ion thruster, this corresponds to a two percent loss in total power efficiency. Such power losses are undesirable on limited power satellites. Another disadvantage was the difficulty in obtaining accurate keeper voltage measurements with the diode in the circuit. Diode voltage drop is a function of temperature. The main cathode keeper voltage is used for closed loop control of the main propellant flow. Variations in the diode voltage drop caused by changes in diode temperature make accurate control difficult. A problem in packaging also existed. It is difficult to provide both a good thermal path for the diodes and electrical insulation for high voltage.

The improved low impedance pulse ignitor eliminates the blocking diode and provides a low resistance path for the keeper current through the secondary of the output transformer during cathode operation. The

low resistance secondary winding was made possible primarily by a sizable reduction in the pulse duration from about 70 microseconds to less than 7 microseconds. A schematic of the pulse ignitor test circuit is shown in figure 2. The rise time of the output pulse voltage was controlled by means of a variable air core inductor in the primary circuit and was made nearly linear by placing a $0.0022 \mu\text{F}$ capacitor across the secondary of the output transformer. The amplitude of the output voltage was controlled by setting the capacitor voltage in the primary circuit. A capacitor voltage in the range of 270 to 320 V, depending on the pulse voltage rise time, generally sufficed to produce a 5 kV peak output, which is presently the limit for the 8-cm EMT system. The output transformer required additional circuitry to reset the core flux level to its starting point after each pulse. The transformer consisted of a magnetic tape wound saturable core with a turns ratio of 30:1. The dc resistance of the secondary was approximately 0.4 ohm. At a neutralizer cathode keeper current of 0.5 A, the power loss is reduced to less than 1/8 W.

Cathodes

The two neutralizer cathodes used in the pulse ignition tests were integral parts of 8-cm ion thruster NIV assemblies which had previously undergone extensive cycle life testing. These NIV assemblies were similar in construction and thermal configuration to the EMT NIV assembly. The cycle life test results are reported in reference 4, where the two NIV's were designated as NIV-1 and NIV-3. Including cycle testing performed subsequent to that reported in reference 4, NIV-1 and NIV-3 completed totals of 4205 and 3825 cycles, respectively. With each cycle including one hour of cathode operation, the total hours of prior cathode operation corresponded approximately to the number of cycles.

Figure 3 shows a cross sectional view of the neutralizer hollow cathode with a design essentially identical to that of the 8-cm EMT cathodes. The cathode consisted of a thin wall 3.2 mm diameter Ta tube with a thoriated tungsten tip, an alkaline earth-oxide coated rolled Ta foil insert, an Al_2O_3 flame-sprayed heater and an enclosed keeper electrode. The cathode tip orifice was 0.25 mm, the keeper orifice diameter was 1.75 mm and the keeper-to-cathode face spacing was 1.5 mm. Other construction details are given in references 4 and 8.

Other than operational characteristics and history, the two cathodes differed only in the kind and amount of alkaline-earth oxide emissive material contained in the rolled foil insert. The NIV-1 insert, which is the same as the EMT insert, was coated with 8 to 10 mg of a double alkaline-earth carbonate consisting of 57 percent BaCO_3 and 43 percent SrCO_3 by weight. The NIV-3 insert was coated with 46 mg of a triple carbonate consisting of 57.2 percent BaCO_3 , 38.8 percent SrCO_3 , and 4.0 percent CaCO_3 by weight.

Figure 4 shows the cathode test configuration. The tests were performed in a multiport vacuum tank where port pressures ranged from a low 10^{-4} torr for high Hg flow rates (60 mA equivalent) to a low 10^{-5} torr for low Hg flow rates (15 mA equivalent). Flow rates were determined by measuring the time rate of change of the Hg column height in a precision bore capillary tube. Hereafter flow rates will be expressed in equivalent mA.

EXPERIMENTAL PROCEDURE

Cathode ignition breakdown voltages were measured for five pulses, each with a different voltage rise time, at cathode tip temperatures estimated to range from approximately 900° to 1130° C and at Hg flow rates of approximately 15, 24, 40, and 60 mA. The maximum amplitude of each pulse was limited to 5 kV. The total rise times for the five pulses to reach 5 kV were 2, 4, 6, 8, and 10 microseconds. The rates of voltage rise were nearly linear, especially between 1 and 4 kV. The open circuit pulse forms are shown in figure 5 and were the same for both cathodes.

Figure 6 shows the power supply arrangement used for the breakdown voltage measurements. The high voltage pulses were applied to the keeper electrode with the dc keeper supply turned off so that after breakdown a discharge was not sustained. This was done in order to observe initial ignition characteristics only and not conditioning effects resulting from cathode operation. Tip heater power was deliberately varied to increase or decrease cathode temperature and thereby raise or lower the breakdown voltage. The vaporizer power was adjusted to maintain a constant Hg flow. Breakdown voltages were measured with the cathodes in thermal equilibrium.

Table I gives some representative steady state NIV cathode tip temperatures for cathode heater powers ranging from 20 to 35 W (ref. 4). These temperatures were determined by means of a thermocouple mounted on the cathode tip of an NIV assembly of identical construction and are assumed equivalent to those of the cathodes under test. The tip temperatures given in table I were measured with the vaporizer temperature corresponding to a cathode starting rate of 24 mA but can be considered as representative for Hg flows between 15 and 60 mA. In this range of flows the cathode tip temperature was observed to be comparatively insensitive to changes in vaporizer heater power.

As shown in figure 7, the low impedance pulser drew a substantial current (approximately 10 A/kV) through the cathode upon breakdown. This resulted in what was assumed to be local heating of the cathode. Consecutive pulses were timed in order to avoid erroneously low breakdown voltages caused by the localized heating effects of previous ignitions. A time delay of two minutes between consecutive pulses was found to be generally sufficient.

RESULTS AND DISCUSSION

Figures 8 to 11 show oscilloscope traces of the breakdown voltages (BDV) for each of the five pulses applied to the NIV-1 cathode (hereafter designated as N1) at Hg flow rates (\dot{m}) of approximately 15, 24, 40, and 60 mA, respectively. Figure 12 shows the BDV for the NIV-3 cathode (hereafter designated as N2) at $\dot{m} = 24$ mA. The pulses are labeled P_1 through P_5 in order of decreasing rate of voltage rise. For each flow rate, the BDV were recorded at four levels of tip heater power (P_H) such that the BDV for the fastest rising pulse ranged from approximately 2 kV up to 5 kV. Correspondingly the BDV for the slowest rising pulse ranged from below 1 kV up to 3.5 kV. The intention was to simulate the range of BDV likely to be encountered during the cycle lifetime of the cathode. Low BDV is characteristic of cathode starting early in its operational lifetime. Because of insert aging effects, commonly observed with the rolled foil insert (refs. 9 and 10), the BDV required for cathode starting increases with time.

Table II presents a tabulation of the BDV for the pulses shown in figures 8 through 12. Also presented are (1) the differences between the BDV of the first four pulses and the BDV of the slowest rising pulse and (2) the average rates of voltage increase ($\Delta V/\Delta t$). The voltage difference is termed "overvoltage" (OV).

Figures 8 through 12 and table II demonstrate the dependence of BDV on rate of voltage rise. This dependence - the faster the voltage rise, the higher the BDV - was consistent with that commonly observed in the impulse voltage breakdown of gases. The BDV rapidly decreased between a pulse with a voltage rise of 2.5 to 3.0 kV/ μ sec (P_1) and a pulse with a voltage rise of 0.3 to 0.5 kV/ μ sec (P_5) for all conditions tested. The effects of changes in tip heater power (hence cathode temperature and level of thermionic emission) on BDV are also illustrated. For example, as shown in figure 9, for N1 at $\dot{m} = 24$ mA, a small increase of 3.4 W (~10 percent) in P_H produced a factor of 2.5 decrease in BDV (from 5 to 2 kV with P_1). This effect was also observed at other Hg flow rates. The P_H requirements for N1, ranging from 36.2 to 39.6 W at $\dot{m} = 24$ mA, were substantially greater than for N2, ranging from 22.3 to 27.0 W at the same Hg flow rate. The large difference in P_H requirements is attributed in part to past handling and more frequent exposure of N1 to a nonvacuum environment (ref. 4).

The plot of BDV against P_H in figure 13 shows that within a narrow range of P_H the BDV for the same pulse does vary significantly with flow. Figure 13 shows that BDV decreases substantially (as much as 2 kV) in going from a flow in the 15 to 24 mA range to a flow in the 40 to 60 mA range. The lower flow rates of 15 and 24 mA are representative of the starting flows for the 8-cm ion thruster neutralizer cathode (typically 24 mA). The higher flow rates of 40 and 60 mA would be more representative of the main cathode which not only has a higher starting flow requirement of 100 to 120 mA but also has a larger keeper orifice diameter of

2.5 mm. Thus the results of this investigation should be applicable to both the main and neutralizer cathodes.

Figure 14 is a plot of the overvoltages for pulses P_1 to P_4 against average rate of voltage rise. There is considerable scatter in the data but the trend is clear. OV increases with $\Delta V/\Delta t$ and becomes quite large (2 kV or more) for the shortest rise time pulse P_1 (2.5 to 3.0 kV/ μ sec).

One theory of overvoltage (ref. 11, p. 117), derived for an ideal case with the rate of voltage rise being strictly linear, states that OV should vary linearly with $(\Delta V/\Delta t)^{1/2}$. In this theory, OV is measured relative to the dc breakdown voltage. Some of the experimental results reported herein showed good agreement with the theory, despite the nonlinearities in the rates of voltage rise and the fact that OV was measured relative to the BDV of the slowest rising pulse P_5 . A good example of this is shown in figure 15, which is a plot of OV against $(\Delta V/\Delta t)^{1/2}$ for N1 at $\dot{m} = 24$ mA. The straight lines connect points for pulses P_1 through P_4 applied under identical conditions. Further comparison of experimental results with theory of the impulse voltage breakdown of gases was precluded by lack of detailed knowledge of important physical parameters.

Figure 16 shows a case where no breakdown occurred for the fastest pulse P_1 but did occur for the other four slower rising pulses. The breakdown for the second fastest pulse P_2 occurred after the pulse had already peaked at 5 kV, suggesting that long pulse duration offers a greater probability for the occurrence of a breakdown. A pulse of long duration ($>5 \mu$ sec) could possibly offset the disadvantage of a very fast rising pulse.

The RESULTS AND DISCUSSION thus far have identified low rate of voltage rise and long pulse duration as desirable pulse characteristics for reliable cathode starting.

Alternate approaches to improving cathode starting reliability, such as increasing the maximum pulse amplitude and raising the cathode temperature, have their limitations. The present 8-cm EMT System design limits the maximum pulse amplitude to 5 kV. Increasing the pulse amplitude further increases electrical insulation and shielding requirements and adds to circuit size and weight. Raising the cathode temperature during startup is an obvious way to reduce the breakdown voltage and will probably be used during the cycle life of the cathodes to maintain the starting breakdown voltage below 5 kV. However, higher cathode temperatures lead to greater thermal stressing of components with increased probability of failure and also to reduced cathode life. There is also a practical limit to the amount of power (36 W for the 8-cm EMT) available for cathode starting.

A flight model pulse ignitor would generate a pulse with a leading edge resembling those of the pulses used in the pulse ignition tests.

Although low rate of voltage rise and long pulse duration are desirable for reliable cathode starting, trade-offs with transformer size and weight must be considered in the design of a flight model pulse ignitor.

A convenient way to view these trade-offs is with a qualitative discussion of the transformer equation below (ref. 12).

$$\int_0^T V_p(t) dt = N_s A_c \Delta B \cdot 10^{-8}$$

Here T is the pulse duration in seconds, $V_p(t)$ is the pulse voltage, N_s is the number of turns in the secondary, A_c is the cross-sectional area of the core in cm^2 and ΔB is the total flux density change in gauss during the pulse. Clearly a low, constant $\Delta V/\Delta t$ and a maximum pulse amplitude of 5 kV could make the volt-second integral on the left side of the equation very large. This would require that the quantity $N_s A_c \Delta B$ also be large. However, it is desirable to minimize transformer size and weight which increase with cross-sectional area, A_c , and number of turns, N_s . One way in which a larger volt-second integral is possible, thereby enabling a greater flexibility in the choice of $\Delta V/\Delta t$ and T , would be to still keep A_c and N_s small but make ΔB large. The core material and method of flux reset determine the maximum flux excursion, ΔB . Core material selection involves a trade-off between B_{max} of the material and circuit and core energy losses. Since the pulse voltage is positive only, the flux excursion must be positive. Two methods can be used for resetting the core back to its original flux level. One method, that used in the pulse ignition tests reported on here, uses external circuitry to reset the core and allows a flux excursion of $2 B_{\text{max}}$ to be obtained. The second method, that selected for the 8-cm EMT pulse ignitor, uses a self-resetting transformer with an air gap, requires no external circuitry, but limits the flux excursion to B_{max} . Selection of the optimum method involves a trade-off between the size and weight of the external reset circuitry and the gain in ΔB .

CONCLUDING REMARKS

Low rate of voltage rise and long pulse duration have been experimentally identified as pulse characteristics desirable for reliable starting of the 8-cm Hg ion thruster cathodes. The results of the high voltage pulse ignition tests indicate that a pulse with a rate of voltage rise of 0.5 to 1 kV/ μsec would be a reasonable choice. The overvoltages for this pulse were not excessively high, amounting to 500 V or less. Further support for this choice comes from the fact that pulse ignitors used in ongoing cycle life tests, where the cathodes have now completed more than 8000 cycles, have rates of voltage rise in this range. Although a low rate of voltage rise and long duration are desirable pulse characteristics for reliable cathode starting, trade-offs with transformer size and weight must be considered in the design of a flight model pulse ignitor.

REFERENCES

1. Hudson, W. R., and Banks, B. A., "An 8-cm Electron Bombardment Thruster for Auxiliary Propulsion," AIAA Paper 73-1131, Oct. 1973.
2. Banks, B. A., et al., "8-cm Mercury Ion Thruster System Technology," AIAA Paper 74-1116, Oct. 1974.
3. Wintucky, E. G., "High Voltage Pulse Ignition of Mercury Discharge Hollow Cathodes," AIAA Paper 73-1140, Oct. 1973.
4. Wintucky, E. G., "Cycle Life Testing of 8-cm Mercury Ion Thruster Cathodes," AIAA Paper 76-986, Nov. 1976.
5. Mantenieks, M. A., and Wintucky, E. G., "5200-Cycle Test of an 8-cm Diameter Hg Ion Thruster," AIAA Paper 78-649, Apr. 1978.
6. Power, J. L., "Planned Flight Test of a Mercury Ion Auxiliary Propulsion System, Part I: Objectives, Systems Descriptions and Mission Operations," AIAA Paper 78-647, Apr. 1978.
7. Herron, B. G., Hyman, J., Jr., and Hooper, D. J., "Development of an 8-cm Engineering Model Thruster System," AIAA Paper 76-1058, Nov. 1976.
8. Wintucky, E. G., "A 20,000-Hour Endurance Test of a Structurally and Thermally Integrated 5-cm Diameter Ion Thruster Main Cathode," AIAA Paper 75-368, Mar. 1975.
9. Mirtich, M. J., "Investigations of Hollow Cathode Performance for 30-cm Thrusters," AIAA Paper 73-1138, Oct. 1973.
10. Newson, D., Charlton, M. G., and Davis, G. L., "Starting Behaviour of Hollow Cathodes Including Multiple Starts," Proceedings of the 3rd European Electric Propulsion Conference, Deutsche Gesellschaft für Luft-und Raumfahrt, Cologne; 1974, pp. 229-232.
11. Meek, J. M., and Craggs, J. D., Electrical Breakdown of Gases, Oxford Clarendon Press, 1953.
12. Staff of Department of Electrical Engineering, Massachusetts Institute of Technology, Magnetic Circuits and Transformers, Massachusetts Institute Technology Press, 1943.

TABLE I. - REPRESENTATIVE NIV CATHODE

TIP TEMPERATURES FOR VARIOUS

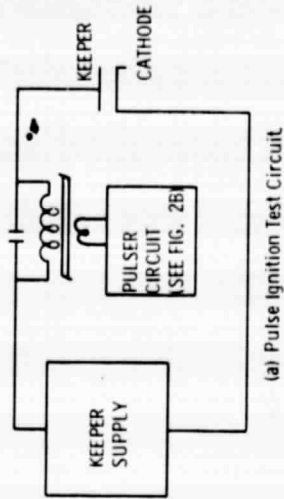
CATHODE HEATER POWER LEVELS

(REF. 4)

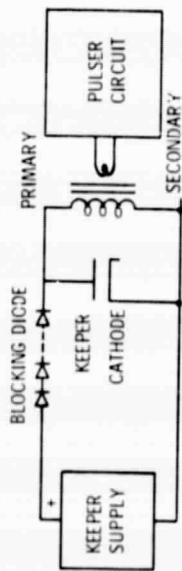
Cathode heater power, W	NIV cathode tip temperature, °C
20	900
25	1000
30	1065
35	1115

TABLE II. - TIP HEATER POWER (P_H), BREAKDOWN VOLTAGE (BDV), OVERVOLTAGE (OV), AND AVERAGE RATE OF VOLTAGE RISE ($\Delta V/\Delta t$) FOR PULSES P_1 TO P_5 SHOWN IN FIGURES 8 TO 12

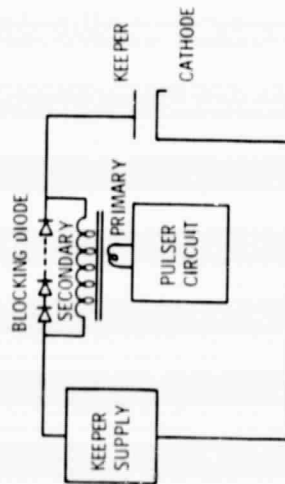
Hg flow rate, mA	Fig.	P_H , W	BDV, kV					OV, kV					$\Delta V/\Delta t$, kV/ μ sec				
			P_1	P_2	P_3	P_4	P_5	P_1	P_2	P_3	P_4	P_5	P_1	P_2	P_3	P_4	P_5
N1	15	36.4	5.0	4.7	4.1	3.8	3.6	1.4	1.1	0.5	0.2	--	2.50	1.47	1.00	0.73	0.55
	8(a)	37.0	4.2	3.0	2.6	2.3	2.1	2.1	.9	.5	.2	--	3.00	1.43	.96	.68	.51
	8(b)	37.7	3.4	2.4	2.0	1.7	1.5	1.9	.9	.5	.2	--	2.83	1.41	.91	.65	.47
	8(c)	39.1	2.4	1.6	1.3	1.1	1.0	1.4	.6	.3	.1	--	2.67	1.14	.72	.50	.38
24	9(a)	36.2	4.9	4.0	3.6	3.4	3.2	1.7	0.8	0.4	0.2	--	2.72	1.43	0.95	0.71	0.52
	9(b)	37.0	4.0	2.8	2.4	2.0	1.7	2.3	1.1	.7	.3	--	3.08	1.40	.89	.63	.45
	9(c)	38.0	2.7	1.8	1.5	1.3	1.1	1.6	.7	.4	.2	--	2.70	1.13	.75	.54	.37
	9(d)	39.6	1.8	1.2	.9	.8	.7	1.1	.5	.2	.1	--	2.25	1.00	.60	.44	.32
40	10(a)	33.7	5.0	4.2	3.5	3.2	3.0	2.0	0.8	0.5	0.2	--	2.63	1.50	0.97	0.73	0.56
	10(b)	35.0	4.0	2.8	2.3	2.0	1.8	2.2	1.0	.5	.2	--	3.08	1.40	.92	.67	.49
	10(c)	36.2	3.0	2.1	1.7	1.6	1.5	1.5	.6	.2	.1	--	3.00	1.40	.85	.67	.50
	10(d)	37.4	2.2	1.5	1.2	1.1	1.0	1.2	.5	.2	.1	--	2.75	1.25	.75	.55	.38
60	11(a)	34.6	4.9	4.2	3.8	3.5	3.3	1.6	0.9	0.5	0.3	--	2.88	1.50	0.97	0.73	0.54
	11(b)	35.0	4.3	3.3	2.8	2.6	2.2	2.1	1.1	.6	.4	--	3.07	1.43	.93	.69	.54
	11(c)	36.4	3.7	2.6	2.2	2.0	1.8	1.9	.8	.4	.2	--	3.08	1.44	.90	.65	.47
	11(d)	37.4	2.3	1.6	1.2	1.1	1.0	1.3	.6	.2	.1	--	2.42	1.10	.62	.46	.35
N2	24	22.3	5.0	4.3	3.8	3.6	3.5	1.5	0.8	0.3	0.1	--	2.94	1.48	0.99	0.71	0.55
	12(a)	23.8	4.0	2.8	2.4	2.3	2.1	1.9	.7	.3	.2	--	3.33	1.40	.91	.68	.51
	12(b)	25.7	2.9	2.0	1.7	1.5	1.4	1.5	.6	.3	.1	--	3.05	1.33	.85	.63	.47
	12(c)	27.0	2.0	1.3	1.1	.9	.8	1.2	.5	.3	.1	--	2.50	1.08	.73	.50	.36



(a) Pulse Ignition Test Circuit



(a) PULSER OUTPUT PARALLEL TO KEEPER SUPPLY (PULSER TRANSFORMER SECONDARY RESISTANCE IS OF ORDER, 500 OHMS).



(b) PULSER OUTPUT IN SERIES WITH KEEPER SUPPLY (PULSER TRANSFORMER SECONDARY RESISTANCE IS OF ORDER, 500 OHMS).

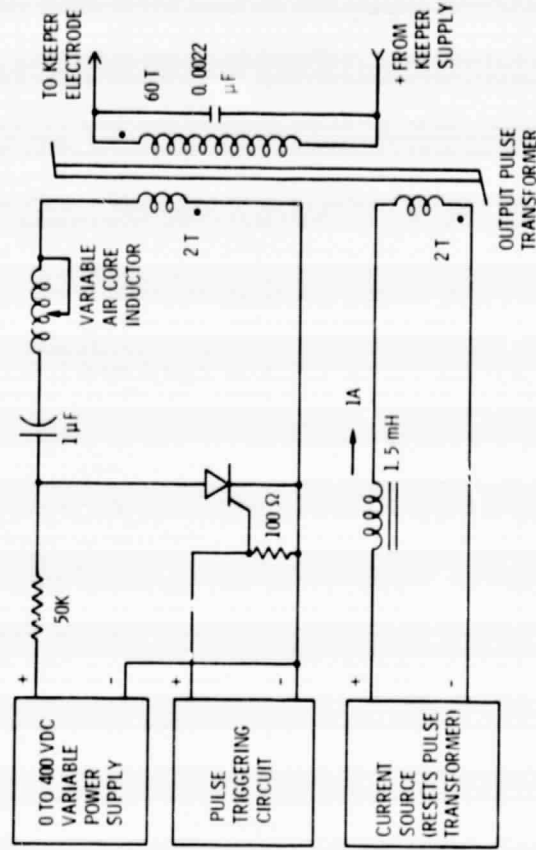
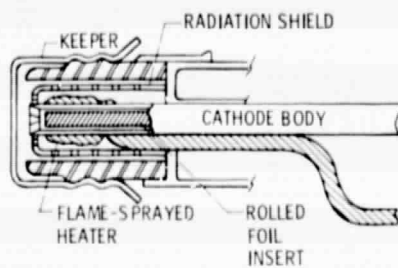


Figure 2bl - Pulse Ignitor Test Circuit

Figure 1. - Two high voltage pulse circuit configurations used previously with blocking diodes in series with keeper supply.



ORIGINAL PAGE IS
OF POOR QUALITY

Figure 3. - Cross-sectional view of neutralizer hollow cathode.

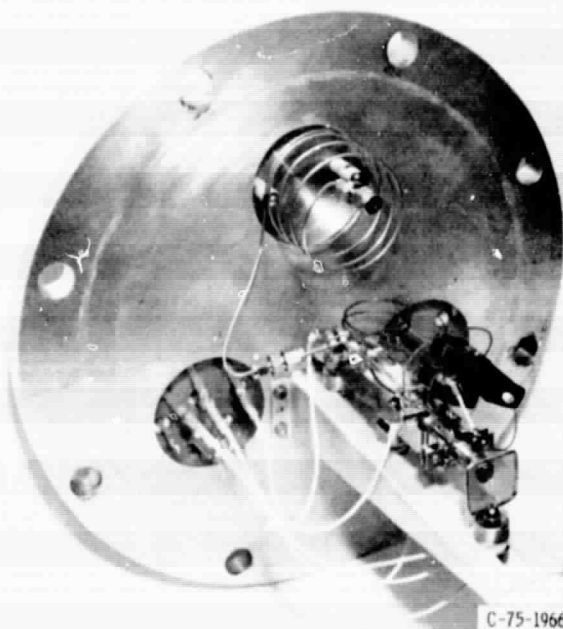


Figure 4. - NIV test configuration in multiport vacuum tank.

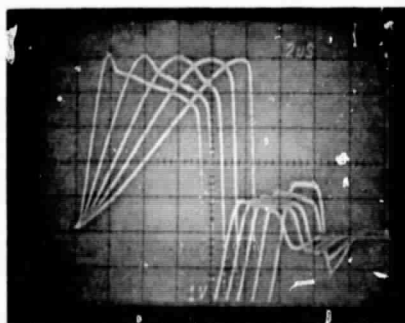


Figure 5. - Oscilloscope traces of the open circuit pulse forms. Vertical scale is 1 kV/div. Horizontal scale is 2 μ sec/div.

ORIGINAL PAGE IS
OF POOR QUALITY

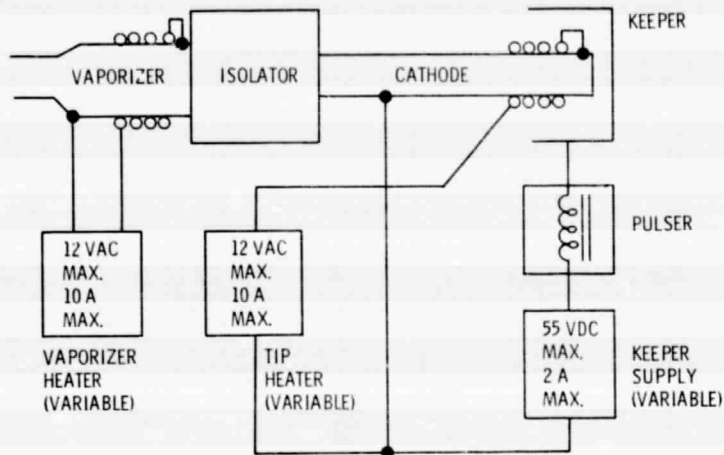
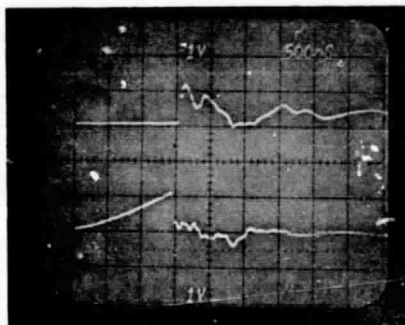
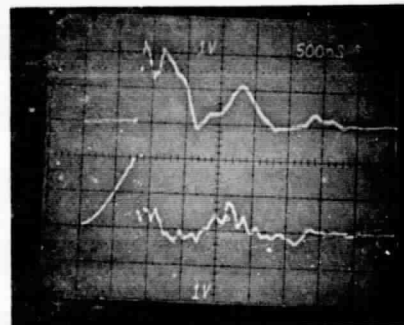


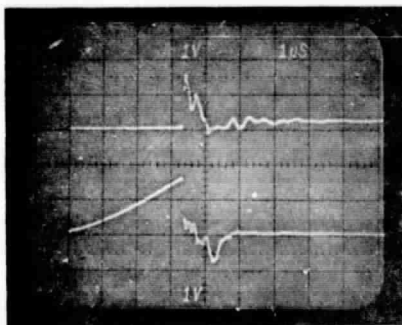
Figure 6. - Power supply arrangement used for breakdown voltage tests.



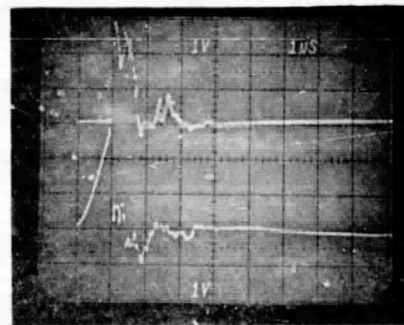
(a) $\dot{m} = 24 \text{ mA}$.



(b) $\dot{m} = 24 \text{ mA}$.

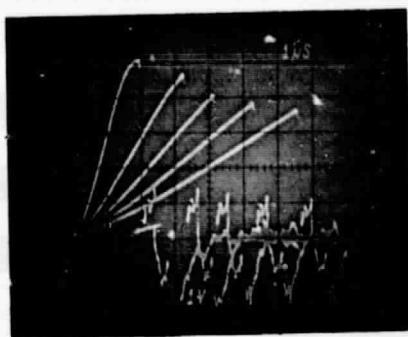


(c) $\dot{m} = 13 \text{ mA}$.

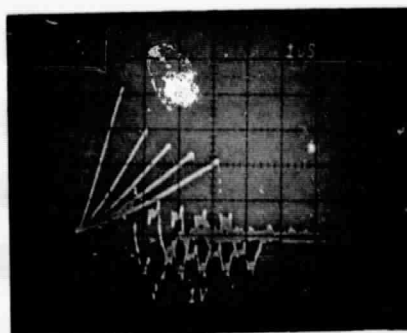


(d) $\dot{m} = 13 \text{ mA}$.

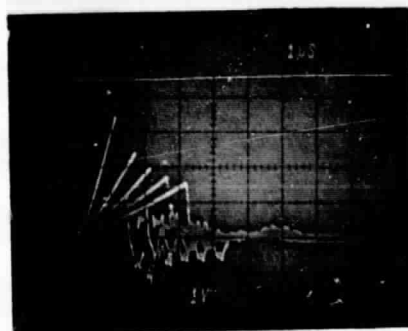
Figure 7. - Oscilloscope traces of breakdown voltages (lower traces) and currents (upper traces) for N₂. Vertical scale is 10 A/div. for current and 1 kV/div. for voltage. Horizontal scale is 0.5 μsec/div. for figures 7(a) and (b) and 1 μsec/div. for figures 7(c) and (d).



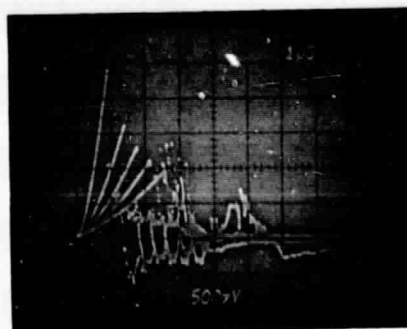
(a) $P_H = 36.4 \text{ W}$.



(b) $P_H = 37.0 \text{ W}$.



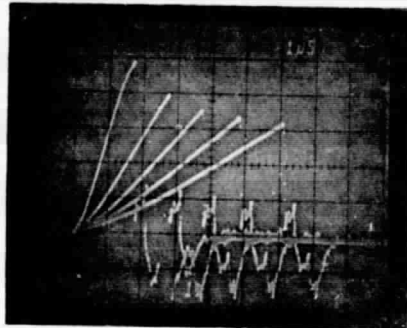
(c) $P_H = 37.7 \text{ W}$.



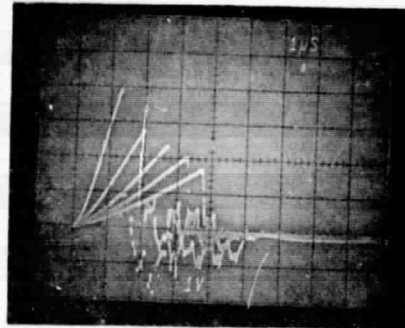
(d) $P_H = 39.1 \text{ W}$.

Figure 8. - Oscilloscope traces of breakdown voltages for pulses P1 through P5 (in order of decreasing rise time) applied to N1 at $\dot{m} = 15 \text{ mA}$. Figures 8(a) through (d) are in order of increasing tip heater power. Vertical scale is 1 kV/div. for figures 8(a) through (c) and 0.5 kV/div. figure 8(d). Horizontal scale is 1 μsec/div.

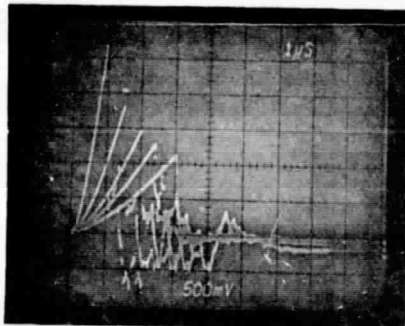
ORIGINAL PAGE IS
OF POOR QUALITY



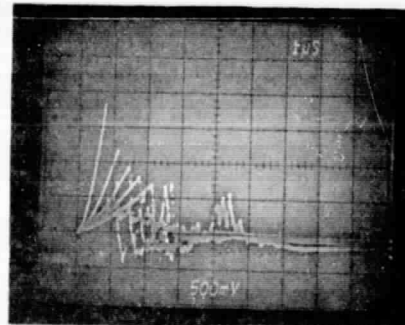
(a) $P_H = 36.2 \text{ W}$.



(b) $P_H = 37.0 \text{ W}$.

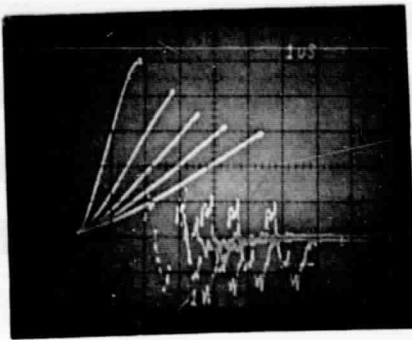


(c) $P_H = 38.0 \text{ W}$.

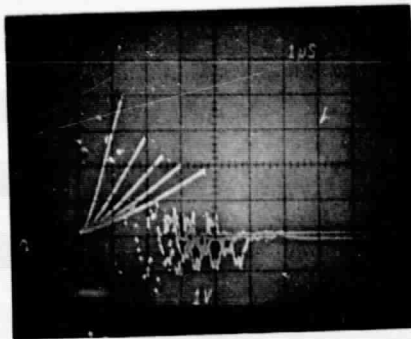


(d) $P_H = 39.6 \text{ W}$.

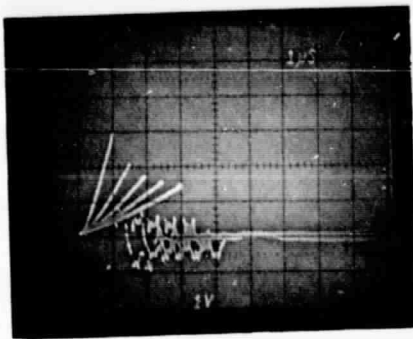
Figure 9. - Oscilloscope traces of breakdown voltages for pulses P1 through P5 (in order of decreasing rise time) applied to N1 at $\dot{m} = 24 \text{ mA}$. Figures 9(a) through (d) are in order of increasing tip heater power. Vertical scale is 1 kV/div. for figures 9(a) and (b) and 0.5 kV/div. for figures 9(c) and (d). Horizontal scale is 1 $\mu\text{sec/div.}$



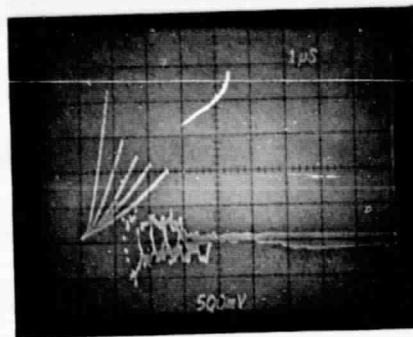
(a) $P_H = 33.7 \text{ W}$.



(b) $P_H = 35.0 \text{ W}$.

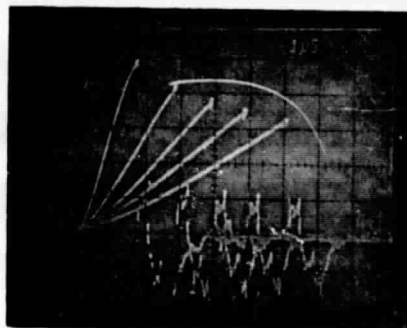


(c) $P_H = 36.2 \text{ W}$.

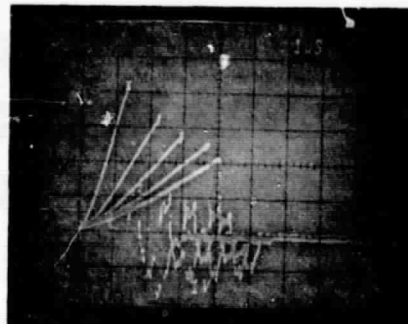


(d) $P_H = 37.4 \text{ W}$.

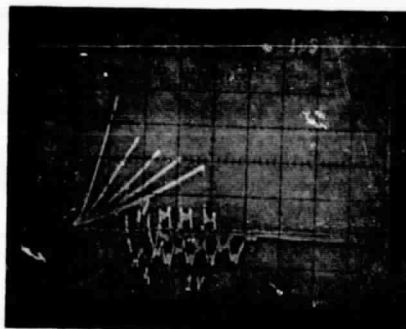
Figure 10. - Oscilloscope traces of breakdown voltages for pulses P1 through P5 (in order of decreasing rise time) applied to Ni at $i_m = 40 \text{ mA}$. Figures 10(a) through (d) are in order of increasing tip heater power. Vertical scale is 1 kV/div . for figures 10(a) through (c) and 0.5 kV/div . for figure 10(d). Horizontal scale is 1 μsec/div .



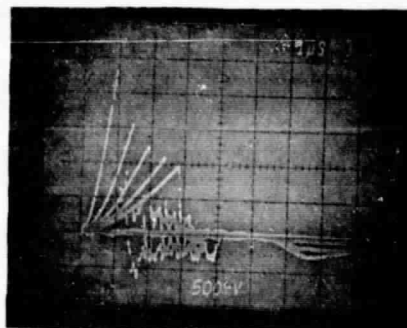
(a) $P_H = 34.6 \text{ W}$.



(b) $P_H = 35.0 \text{ W}$.



(c) $P_H = 36.4 \text{ W}$.



(d) $P_H = 37.4 \text{ W}$.

Figure 11. - Oscilloscope traces of breakdown voltages for pulses P1 through P5 (in order of decreasing rise time) applied to N1 at $i_m = 60 \text{ mA}$. Figure 11(a) through (d) are in order of increasing tip heater power. Vertical scale is 1 kV/div . for figure 11(a) through (c) and 0.5 kV/div . for figure 11(d). Horizontal scale is $1 \mu\text{sec/div}$.

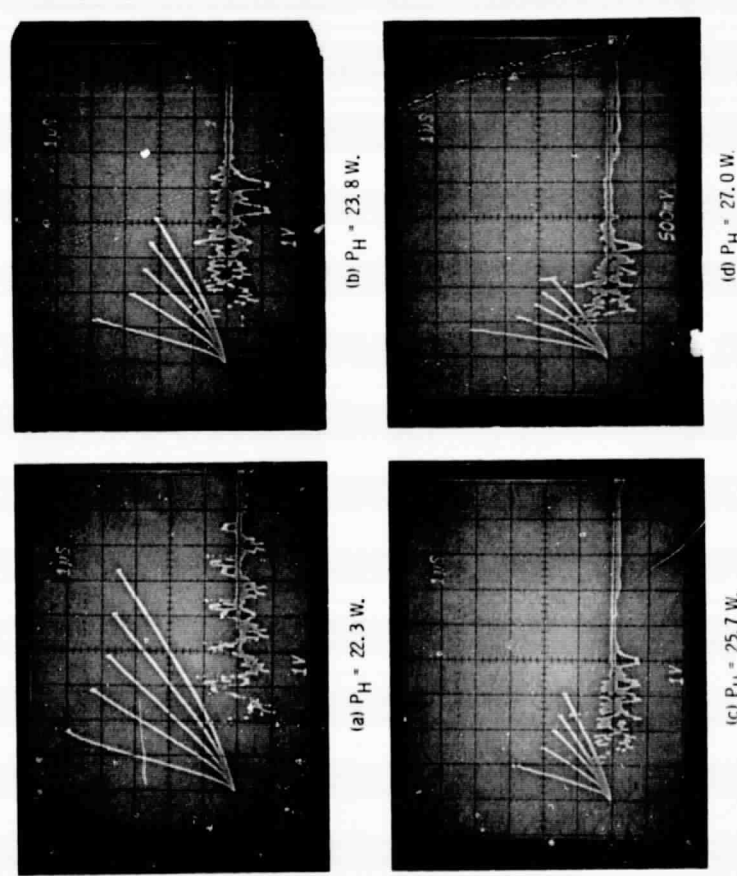


Figure 12. - Oscilloscope traces of breakdown voltages for pulses P1 through P5 (in order of decreasing rise time) applied to N2 at $i_m = 24$ mA. Figures 12(a) through (d) are in order of increasing tip heater power. Vertical scale is 1 kV/div. for figures 12(a) through (c) and 0.5 kV/div. for figure 12(d). Horizontal scale is 1 μ s/div.

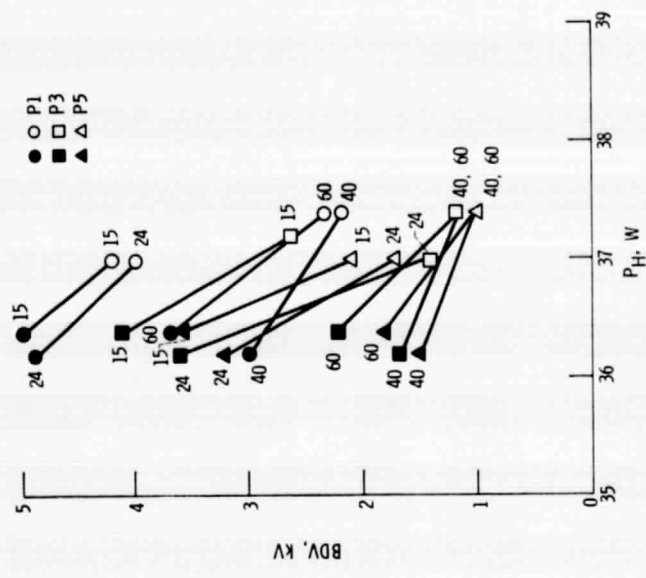


Figure 13. - Breakdown voltage (BDV) vs tip heater power (P_H) for pulses P1, P3, and P5 with N1 cathode. Numbers by symbols indicate Hg flow rates. Compare solid symbols of the same kind and open symbols of the same kind.

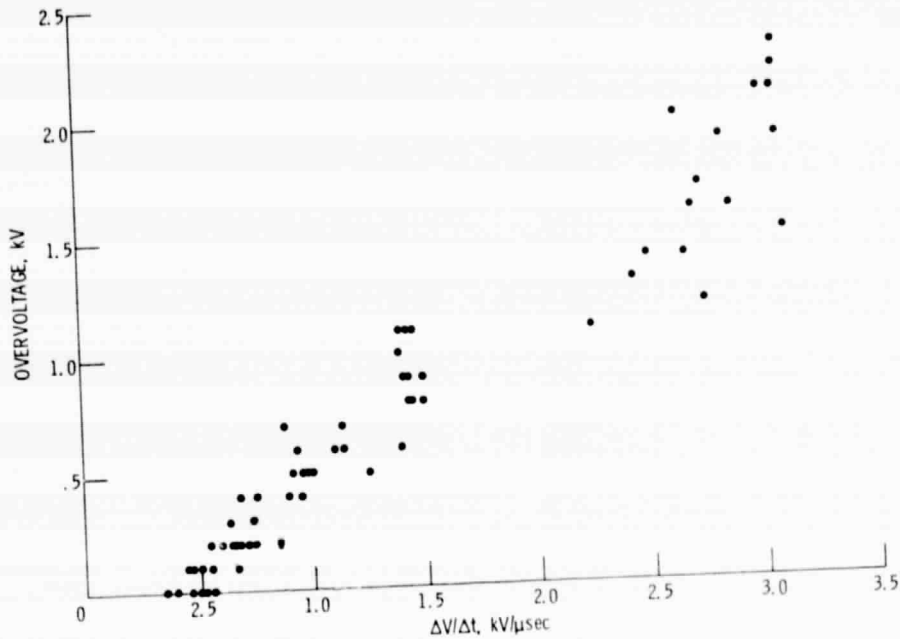


Figure 14. - Overvoltage vs average rate of voltage rise ($\Delta V/\Delta t$).

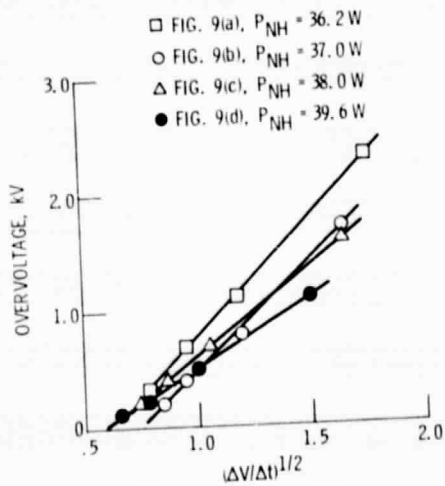


Figure 15. - Overvoltage vs $(\Delta V/\Delta t)^{1/2}$ for N1 at 24 mA Hg flow. Each straight line connects points for pulses P1 thru P4 applied under identical conditions.

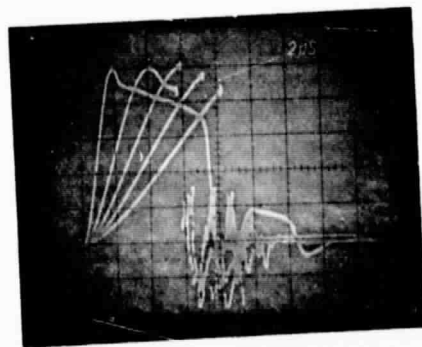


Figure 16. - Oscilloscope traces for pulses P1 through P5 applied to N1 showing no breakdown for the fastest voltage rise pulse, P1. Vertical scale is 1 kV/div. Horizontal scale is 2 μ sec/div.